

Mirko Blagojevic

Professor
e-mail: mirkob@kg.ac.rs

Nenad Marjanovic

Professor
e-mail: nesam@kg.ac.rs

Zorica Djordjevic

Professor
e-mail: zoricadj@kg.ac.rs

Blaza Stojanovic

Assistant Professor
e-mail: blaza@kg.ac.rs

Faculty of Mechanical Engineering,
Kragujevac, Serbia

Aleksandar Disic

Assistant Professor
Institute for Vehicles Zastava,
Kragujevac, Serbia
e-mail: aleksandardisic@gmail.com

A New Design of a Two-Stage Cycloidal Speed Reducer

A new design of a two-stage cycloidal speed reducer is presented in this paper. A traditional two-stage cycloidal speed reducer is obtained by the simple combination of single-stage cycloidal speed reducers. A single-stage reducer engages two identical cycloid discs in order to balance dynamical loads and to obtain uniform load distribution. Consequently, the traditional two-stage reducer has four cycloid discs, in total. The newly designed two-stage cycloidal speed reducer, presented in this paper, has one cycloid disc for each stage, that is, two cycloid discs in total, which means that it is rather compact. Due to its specific concept, this reducer is characterized by good load distribution and dynamic balance, and this is described in the paper. Stress state analysis of cycloidal speed reducer elements was also realized, using the finite elements method (FEM), for the most critical cases of conjugate gear action (one, two, or three pairs of teeth in contact). The results showed that cycloid discs are rather uniformly loaded, justifying the design solution presented here. Experimental analysis of the stress state for cycloid discs was realized, using the strain gauges method. It is easy to conclude, based on the obtained results, that even for the most critical case (one pair of teeth in contact) stresses on cycloid discs are in the allowed limits, thus providing normal functioning of the reducer for its anticipated lifetime. [DOI: 10.1115/1.4004540]

1 Introduction

In accordance with modern development trends in the area of complex machine constructions, high power transmission gears with high transmission ratios and low losses are becoming a necessity. Considering the limitations imposed on standard transmission gears in regards to their power and dimensions, planetary gears have started to be applied as a substitution for complex transmission gears.

The cycloidal speed reducer belongs to a group of new generation planetary gears. They are broadly used in the modern industry. The most common applications are in the areas of robot industry, satellite technology, tool machines, elevators, the process industry, transporters, etc. Cycloidal speed reducers have found a broad use due to a number of excellent characteristics they possess such as long and reliable work life, large range of possible transmission ratios, extremely reliable functioning in dynamical load conditions, compact design, and high efficiency coefficient.

Basic information about cycloidal speed reducers and the means of profile generation for cycloid disc teeth, as well as for elements loading is given in Refs. [1–3]. Litvin [4] studied the surface geometry of some particular conjugate gear pairs. Blanche and Yang [5,6] analyzed the effects of machining tolerances on backlash and torque ripples. Pin gearing can be an antibacklash gear for some special applications [7]. Modification of rotor profile geometry for a cycloidal pump is analyzed in Ref. [8]. Litvin and Feng [9] analyzed the generation and geometry of planar cycloidal gearings and improved the design which eliminated profile and surface singularities. A profile modification of cycloid disc teeth is realized in order to achieve better working characteristics of cycloidal gearings in Ref. [10]. These modifications significantly influence the distribution of forces, stress, and deformations on reducer elements. Chmurawa and John [11] have performed stress–strain analysis of cycloid discs with a modified profile using finite elements method (FEM). Yan and Lai [12] developed a cycloidal speed reducer with cylindrical tooth-profiles and derived the equation of meshing. One tooth difference

cycloid drives are most commonly used today. Chen et al. [13] investigated the cycloid drives when the tooth difference numbers between ring gear and cycloid disc are 1, 2, 3, and -1 . Hwang and Hsieh [14] derived a mathematical model with tooth difference for two types of cycloidal profile: pin wheel epitrochoid meshing and pin wheel hypotrochoid meshing. Based on contact force and curvature analysis, they concluded that the pin wheel hypotrochoid meshing design has better characteristics. They also derived dimensionless equations of nonundercutting for a cycloidal speed reducer and gerotor [15]. Meng et al. [16] derived a mathematical model of a cycloidal speed reducer including friction. Sensinger [17] developed a method for a cycloid drive profile for stress and efficiency optimization. The dynamic behavior of a cycloidal speed reducer is presented in Refs. [18–20].

There is a constant tendency to adopt new design solutions in order to improve the working characteristics of a cycloidal reducer (efficiency coefficient, transmission ratio, dimensions, etc). A double crank ring-plate-type cycloid drive which is able to transfer larger torque than a typical existing planetary cycloid drive is presented in Ref. [21]. Gorla et al. [22] developed a new type of cycloidal speed reducer with an external ring gear and cylindrical rollers mounted on the cycloid disc. They derived a procedure for calculating the contact forces on cycloid drive elements, power losses, and theoretical mechanical efficiency. An innovative design of epicyclic (planetary) cam trains based on pure-rolling contact is presented in Ref. [23].

The two-stage cycloidal speed reducer of a new design is presented in this paper. The procedure for calculation of loads acting on its elements is described. Stress state analysis of vital elements of the reducer is also realized, using numerical and experimental methods.

2 Traditional and New Concept of a Two-Stage Cycloidal Speed Reducer

An exploded view of a one-stage cycloidal speed reducer of traditional design is shown in Fig. 1, where two cycloid discs, relatively turned to each other for an angle of 180° , are used for each stage. The working principle is as follows: eccentric (2) is rotating with the same number of revolutions and in the same direction as the input shaft (1). Cycloid discs (4) are situated on the eccentric

Contributed by the Power Transmission and Gearing Committee of ASME for publication in the JOURNAL OF MECHANICAL DESIGN. Manuscript received September 25, 2010; final manuscript received June 22, 2011; published online August 8, 2011. Assoc. Editor: Prof. Philippe Velex.

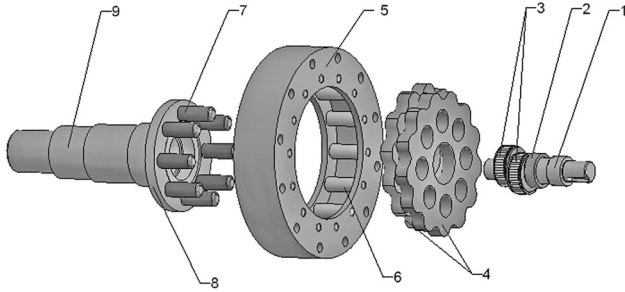


Fig. 1 A single-stage cycloidal speed reducer

through bearings (3). Cycloid discs are conjugated with ring gear rollers (6) located within the body of the ring gear (5). The result of this conjugation is the complex motion of the cycloid discs consisting of a rotation that originates from the eccentric, in the direction of the input shaft rotation and rotation of cycloid discs around their own axes in the opposite direction. Output rollers (7), whose carrier (8) is tightly connected to the output shaft (9), go through the circular openings of the cycloid discs and transfer their motion to the output shaft.

A multistage cycloidal speed reducer is obtained by the combination of single-stage cycloidal reducers. Input and output shafts are rotating in opposite directions at single-stage and three-stage cycloidal reducers, while at two-stage reducers these two shafts have the same revolving direction. A two-stage cycloidal speed reducer of traditional design is presented in Fig. 2.

It is obvious from Fig. 2 that the two-stage cycloidal speed reducer of traditional design is made by the simple combination of two single-stage cycloidal speed reducers. The output shaft of the first stage is at the same time input shaft of the second stage. Taking into account that for each stage two identical cycloid discs are used, rotated in respect to each other by the angle of 180° , in order to obtain uniform load distribution, it means that the traditional two-stage cycloidal reducer has four cycloid discs in total.

A two-stage cycloidal speed reducer of a completely new concept is presented in this paper. The concept is developed with an objective to lower the reducer's dimensions and to retain all its good character-

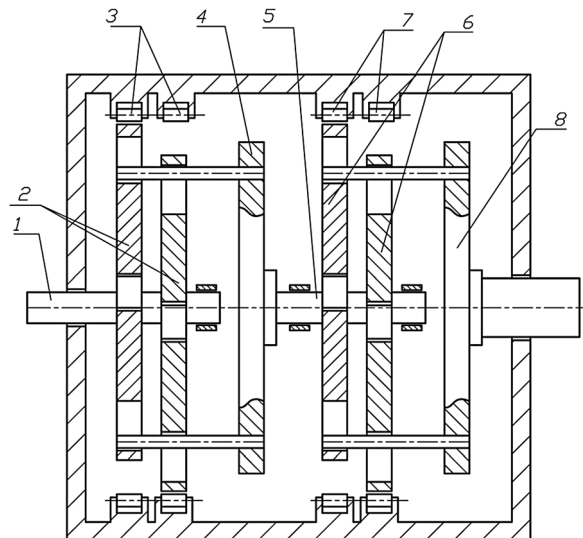


Fig. 2 The traditional design of a two-stage cycloidal speed reducer (1—input shaft with the eccentric (the first stage), 2—the first stage cycloid discs, 3—stationary ring gear of the first stage, 4—output disc of the first stage with output rollers and output shaft, 5—input shaft with the eccentric (the second stage), 6—the second stage cycloid discs, 7—stationary ring gear of the second stage, 8—output disc of the second stage with output rollers and output shaft)

istics. The need for this type of reducer is mostly pronounced in the robot industry. Schematic representation of the new design of the two-stage cycloidal speed reducer is shown in Fig. 3.

The working principle of this cycloidal speed reducer is different from the traditional one. Only one cycloid disc is used for each stage. The complex motion of the first stage cycloid disc (2) is realized during the turning of the input shaft of the reducer (1). The cycloid disc (2) is in contact with the housing rollers of the stationary ring gear of the first stage (3) and can freely rotate around its own axis.

The rollers of the central disc (4) pass through the openings in the cycloid disc (2). The central disc rotates in an opposite direction to that of the input shaft and can freely rotate around the shaft axis. Its rollers do not only pass through the openings in the first stage cycloid disc, but also through the openings in the second stage cycloid disc (5). Due to this type of relation between these two cycloid discs, they both revolve in the same direction. The input shaft of the second stage is rotating with the same angular velocity as the input shaft of the first stage. This concept is different from the traditional one where the cycloid disc and ring gear are both rotating. However, their conjugation is enabled by the rollers of the central disc (4) which represent solid support. The ring gear of the second stage (6) actually receives the resulting motion and the torque. The ring gear (6) is tightly connected to the output shaft of the reducer and rotates in the same direction as the input shaft.

The main idea of the new concept is that the cycloid disc (5) with the central disc (4) and ring gear (6) has switched their roles. A disassembled computer model of the reducer is shown in Fig. 4. A photo of the designed and manufactured two-stage cycloidal speed reducer of the new design is presented in Fig. 5.

Unlike the traditional, two-stage cycloidal speed reducer with four cycloid discs in total, the newly developed concept has only two cycloid discs, thus providing a significantly more compact design. If the two-stage cycloidal speed reducer of the new design is compared to the one-stage cycloidal speed reducer with the same transmission ratio, input power, and input speed, the following can be concluded:

- The newly designed two-stage cycloidal speed reducer has significantly fewer rollers than the one-stage cycloidal speed reducer. This could have substantial advantages in lowering the required stress (due to increase of the rollers' diameter) and allowing for an increased cam offset.
- The housing dimensions of these two cycloidal speed reducers are almost identical (Figs. 1 and 4).

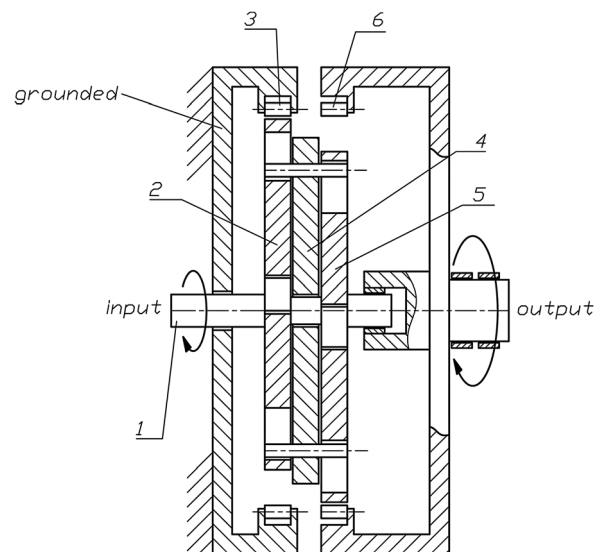


Fig. 3 The kinematic scheme of the newly designed two-stage cycloidal speed reducer

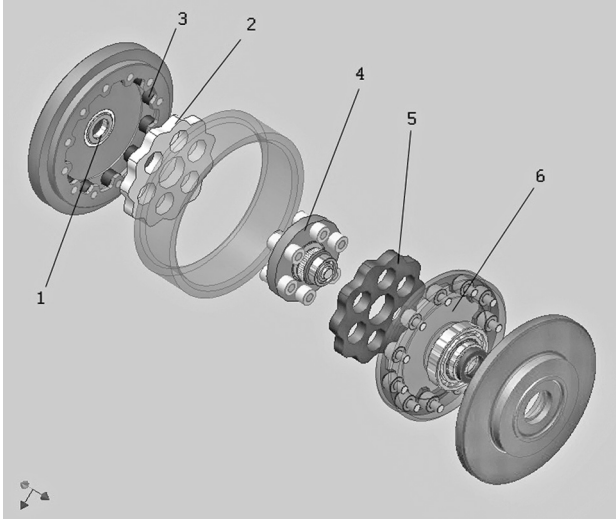


Fig. 4 A disassembled two-stage cycloidal speed reducer of the new design

- There are fewer moving parts on the newly designed two-stage cycloidal speed reducer, so the drive will likely be less noisy.
- The cycloid disc of the second stage vibrates eccentrically, too. In this way, it is canceling out the eccentric vibrations of the first cycloid disc (as with the traditional cycloidal speed reducer).

3 Loads at the Cycloidal Speed Reducer and Transmission Ratio

Taking into account that this is a completely new concept of the two-stage cycloidal speed reducer, torque distribution on the reducer elements cannot be completely applied as known according to the literature, such as in Refs. [1–3,10,20,21]. The basic characteristics of the new concept are as follows:

1. The first and the second stage have a common input shaft.
2. For each stage, only one cycloid disc is used.
3. The cycloid discs of the first and second stage are connected to each other by the central disc rollers.
4. The cycloid disc and ring gear are both rotatable at the second stage. However, their conjugation is enabled by the rollers of the central disc (4) which represent solid support.



Fig. 5 A photo of the manufactured physical model of the cycloidal speed reducer

All the losses in the reducer are neglected, because the main objective of this paper is the definition and analysis of the theoretical model of the two-stage cycloidal speed reducer of the new concept.

3.1 Torque. Drive torque–electromotor torque (T_{EM}) is divided into two parts as:

- Drive torque of the first stage, T_{I1} ,
- Drive torque of the second stage, T_{I11}

$$T_{EM} = T_{I1} + T_{I11} \quad (1)$$

Interrelation of the drive torques of the first and second stage depends on the first transmission ratio u_1 and is defined by the expression

$$T_{I11} = T_{I1} \cdot u_1 \quad (2)$$

Reducer's output torque is equal to the torque on the ring gear of the second stage, T_{I12} , as

$$T_{I12} = T_{EM} \cdot u_1 \cdot u_2 \quad (3)$$

u_2 —the second transmission ratio.

Taking into account the connection of the cycloid discs of the first and the second stage, the following equation is valid:

$$T_{I3} - T_{I13} = 0 \quad (4)$$

where T_{I3} is torque on the first stage cycloid disc and T_{I13} is torque on the second stage cycloid disc.

Torque balance equation for the first stage cycloid disc is given by the following expression [10,11]:

$$T_{I1} - T_{I2} + T_{I3} = 0 \quad (5)$$

T_{I2} —torque on the stationary ring gear of the first stage.

For the second stage, the following balance equation is valid:

$$T_{I11} + T_{I12} - T_{I13} = 0 \quad (6)$$

T_{I12} —torque on the rotatable ring gear of the second stage.

By arranging Eqs. (1)–(6), the following system of equations is obtained:

$$T_{I1} = \frac{T_{EM}}{u_1 + 1} \quad (7)$$

$$T_{I2} = T_{EM}(1 + u_1 \cdot u_2) \quad (8)$$

$$T_{I3} = T_{EM} \cdot u_1 \cdot \left(\frac{1}{1 + u_1} + u_2 \right) \quad (9)$$

$$T_{I11} = \frac{T_{EM} \cdot u_1}{1 + u_1} \quad (10)$$

$$T_{I12} = T_{EM} \cdot u_1 \cdot u_2 \quad (11)$$

$$T_{I13} = T_{EM} \cdot u_1 \cdot \left(\frac{1}{1 + u_1} + u_2 \right) \quad (12)$$

Considering the completely new torque distribution, cycloid discs of the first and second stage are almost uniformly loaded, and this contributes to good dynamical balance of the reducer as in the case of the traditional concept. In this way, the effect achieved with two cycloid discs is almost the same as the effect achieved with classic two-stage cycloidal reducers which use four cycloid discs. This, in return, significantly contributes to a decrease of reducer dimensions, which can easily be seen by comparing Figs. 2 and 3.

In the case of the traditional concept, balancing of the centrifugal forces is obtained by using two identical cycloid discs, relatively turned to each other for an angle of 180°, for each stage. This is not performed in the case of the new concept. However, balancing of centrifugal forces is provided by cycloid discs of the first and second stage also being turned for 180°. Furthermore, their torques are equal (losses are not taken into account), and their geometrical characteristics are also similar.

3.2 Contact Forces. In a theoretical case, all teeth of the cycloid disc are in contact with the corresponding rollers of the ring gear and half of them transfer load. A calculation procedure for this case is presented in detail in Refs. [1–3, 21]. However, this is not the case in real practice, because certain clearances exist between the rollers of the ring gear and the teeth of the cycloid disc in order to compensate errors made during the manufacturing process of the cycloid disc, to provide better conditions for lubrication, to accomplish easier assembling and disassembling of the reducer, and so on. The size of these clearances directly influences the distribution of the contact forces that appear in contact between the cycloid disc teeth and ring gear rollers. It means that with the increase of clearances' size, the number of corresponding elements that transfer load is decreasing. In this paper, machining tolerances have been taken into account only for the contact forces. The cycloid disc in contact with the ring gear rollers and output rollers is presented in Fig. 6.

Values of the contact forces depend on the size of clearances, that is, on the number of cycloid disc teeth (rollers of the ring gear) that transfer load.

Torque on the ring gear can be calculated as

$$T_2 = \sum_{i=1}^n F_{Ni} \cdot r_i \quad (13)$$

where F_{Ni} is contact forces that appear between the cycloid disc teeth and ring gear rollers and r_i is normal distances between the centre of the cycloidal reducer R and the corresponding contact forces.

The following relation is valid between contact forces F_{Ni} (F_{Nk}) and corresponding distances r_i (r_k)

$$\frac{F_{Ni}}{F_{Nk}} = \frac{r_i}{r_k} \quad (14)$$

Equation (14) represents one approximative approach to contact forces' calculation derived from the work of Malhotra [3]. This approach is satisfactory enough for the relevance of results.

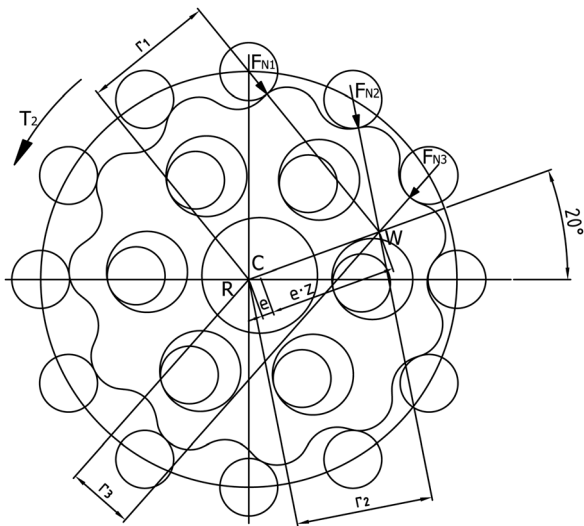


Fig. 6 The first stage cycloid disc

Table 1 Approximate values of contact forces F_{Ni}

Number of pairs of teeth in contact	F_{N1} , N	F_{N2} , N	F_{N3} , N
1 (1st stage)	5091	–	–
2 (1st stage)	2432	2543	–
3 (1st stage)	2166	2265	1098
1 (2nd stage)	5278	–	–
2 (2nd stage)	2378	2625	–
3 (2nd stage)	2006	2215	1287

When there are clearances in the cycloidal speed reducer, approximate values of the contact forces can be calculated, based on Eqs. (13) and (14). For instance, when three pairs of teeth are in contact, contact forces are equal to

$$F_{N1} = \frac{T_2 \cdot r_1}{r_1^2 + r_2^2 + r_3^2}$$

$$F_{N2} = F_{N1} \cdot \frac{r_2}{r_1}$$

$$F_{N3} = F_{N1} \cdot \frac{r_3}{r_1}$$

Distances r_i are calculated based on the expressions described in detail by Malhotra [3]

$$r_i = r_a \cdot \sin(\alpha_i - z \cdot \theta) \quad (15)$$

where r_a is base circle radius of the cycloid disc, α_i is angle which force F_{Ni} makes with the vertical direction, z is cycloid disc number of teeth, and θ is cycloid disc angle of rotation.

3.3 Transmission Ratio. The first stage transmission ratio is calculated based on the following expression [1–3]:

$$u_1 = -\frac{z_{11}}{z_{12} - z_{11}} \quad (16)$$

where z_{11} is the number of teeth of the first stage cycloid disc and z_{12} is the number of rollers of the stationary ring gear of the first stage.

The second stage transmission ratio is calculated based on the following expression:

$$u_2 = -\frac{z_{12}}{z_{112} - z_{111}} \quad (17)$$

where z_{111} is the number of teeth of the second stage cycloid disc and z_{112} is the number of rollers of the rotatable ring gear of the second stage.

In the case of “one tooth difference” cycloidal drive ($Z_{12} - Z_{11} = 1$, $Z_{112} - Z_{111} = 1$), as is the case here, the final expression for the speed reducer ratio u_{CR} is

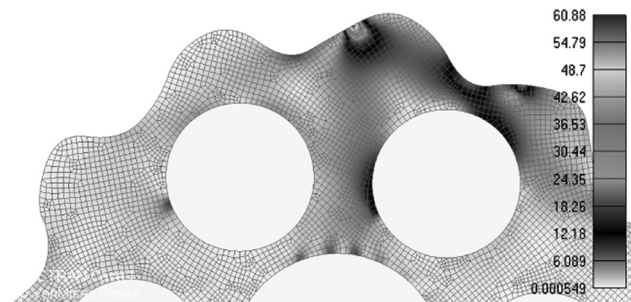


Fig. 7 Von-Mises stress distribution on the first stage cycloid disc—three pairs of teeth in contact

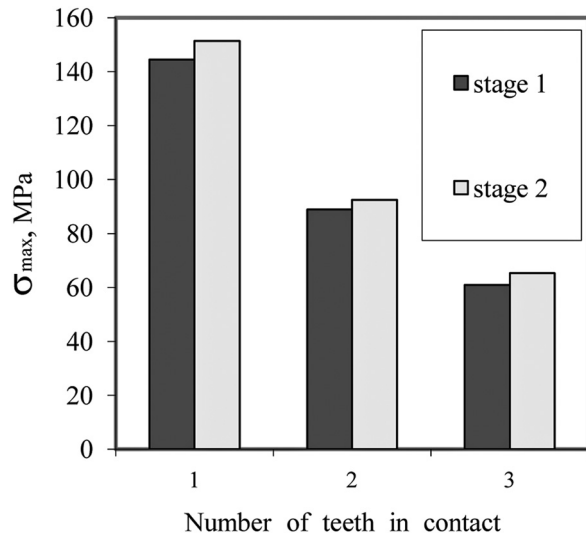


Fig. 8 Values of maximum Von-Mises stress on cycloid discs

$$u_{CR} = Z_{I1} \cdot Z_{II2} \quad (18)$$

The overall transmission ratio has a positive sign, which means that the output shaft rotates in the same direction as the input shaft.

4 Results and Discussion

Stress state analysis of vital elements of the new concept two-stage cycloidal speed reducer was realized using numerical and experimental methods. The basic characteristics of the designed reducer are as follows: $P_{EM} = 0.25$ kW, $n_{EM} = 1390$ min⁻¹, $z_{I1} = 11$, and $z_{II2} = 11$.

The physical model of this reducer is manufactured in the Laboratory for Machine Elements at the Faculty of Mechanical Engineering, Kragujevac. The disassembled reducer is shown in Fig. 5. The physical model confirmed the working principle as well as the value of the transmission ratio.

The influence of machining tolerances on load distribution was taken into account with consideration of the fact that it is a real cycloidal reducer. Based on Eqs. (7)–(12), the calculation of torques on some elements of the reducer was performed. Then, based on Eqs. (13) and (14), approximate values of contact forces F_{Ni} were calculated, in cases where there was one pair or two or three pairs of teeth in contact, for the first and second stage (Table 1).

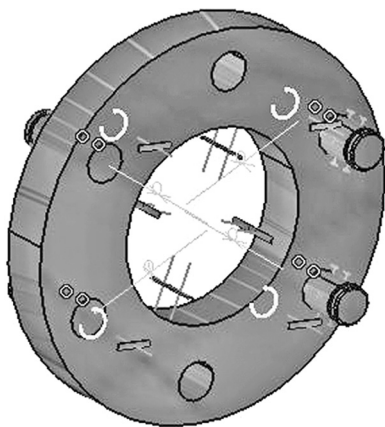


Fig. 9 Central disc (loads and constraints)

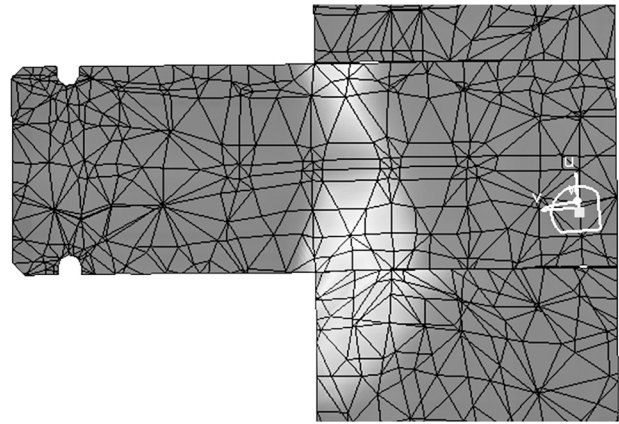


Fig. 10 Stationary ring gear pin (contact stress)

4.1 Stress State Analysis of Cycloidal Speed Reducer Elements Using FEM.

Numerical analysis of the stress state of cycloidal speed reducer elements was realized using software FEMAP and CATIA. First, the cycloid discs of the first and second stage were analyzed. Values of the contact forces were taken from Table 1. The whole series of different 2D models were made, depending on external load (one, two, or three pairs of teeth in contact). Cycloid discs were considered to be elastic, deformable bodies. The whole problem was considered as planar due to the nature of the loads. Analysis was performed in software FEMAP. External loads were contact forces given in appropriate nodes. Stationary supports were placed at the contact of the needle bearing balls with the central opening of the cycloid disc, as well as at the contact of the central disc rollers and appropriate openings in the cycloid disc (these are two upper openings in Fig. 7). Stress-strain state analysis of the cycloid disc was realized for the position of the cycloid disc as given in Fig. 6. Appropriate geometrical values, as well as the values of the contact forces, changed during rotation of the cycloid disc. Based on the results of numerical analysis for different positions of the cycloid disc, presented in Ref. [18], this position can be considered as one of the most critical positions.

The model of the first stage cycloid disc consists of 9227 two-dimensional isoparametric finite elements and 9753 nodes, while the model of the second stage cycloid disc consists of 9200 two-dimensional isoparametric finite elements and 9731 nodes. The values of maximum Von-Mises stress on the cycloid discs of the first and second stage for one, two, and three pairs of teeth in contact are presented in Fig. 8.

Afterwards, numerical analysis of the stress state was performed for other elements of the reducer: central disc, stationary ring gear of the first stage, rotatable ring gear of the second stage,

Table 2 The values of Von-Mises stress on the elements of the two-stage cycloidal speed reducer

Element	Von-Mises stress(MPa)		
	One pair of teeth (rollers) in contact	Two pairs of teeth (rollers) in contact	Three pairs of teeth (rollers) in contact
Cycloid disc—1st stage	144.5	89	60.9
Cycloid disc—2nd stage	151.4	92.4	65.3
Central disc	211	113	74.4
Stationary ring gear of the first stage	122	81.2	58.8
Rotatable ring gear of the second stage	147	75.5	54.7
Eccentric		129	

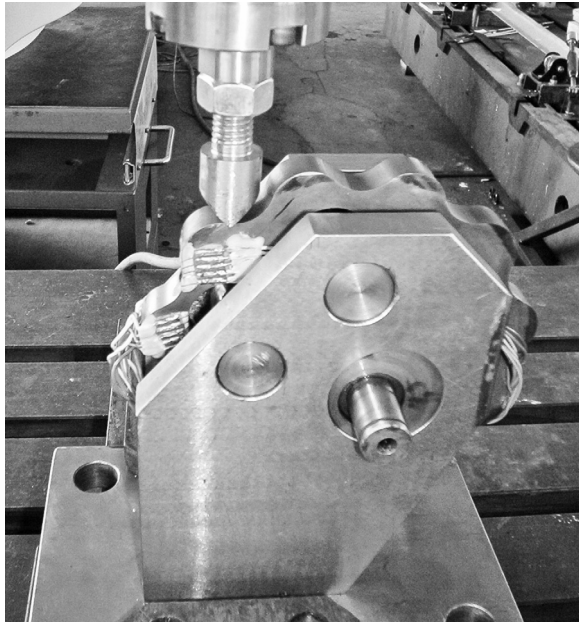


Fig. 11 Model for experimental analysis at the testing table

Table 3 Characteristics of the tested cycloid disc

Number of teeth	$z = 11$
Material	20MoCr4 steel, nitration, grinding
Width	$B = 13.3$ mm
Dedendum diameter	$d_f = 116$ mm
Addendum diameter	$d_a = 132$ mm
Eccentricity	$E = 4$ mm

and the eccentric. Analysis was performed in software CATIA. Three-dimensional curvilinear tetrahedral finite elements were used. The influence of the machining tolerances was also taken into account for these elements, and a number of numerical models were made. The results of this analysis are shown in Figs 9 and 10. All analyzed elements are made of 20MoCr4 steel.

Comparative values of maximum Von-Mises stress on all elements of the two-stage cycloidal speed reducer that were the subject of numerical analysis are presented in Table 2.

4.2 Experimental Analysis. Experimental analysis of the stress state of the first stage cycloid disc, in static working conditions, was realized in order to verify the numerically obtained results. Testing was carried out at SHENK–PVQ 0082 device. The precision class of the measuring device (UPM 60) is 0.02%. The cycloid disc was made for testing purposes, with relevant

positions and a carrier which connects all elements into one unit, in order to better simulate conjugate conditions. The case of single-meshing was analyzed. The presser was acting in the contact zone between the cycloid disc tooth and ring gear roller (Fig. 11). Characteristics of the tested cycloid disc are given in Table 3.

Maximum stresses on the cycloid disc were obtained at its contact with the ring gear rollers, central disc rollers, and rollers of the needle bearings. Due to the extremely favorable shape of the cycloid disc tooth, bending stresses at the base of the tooth could be neglected. Contact stresses were within allowable limits, due to the mainly concave–convex contact between the conjugate surfaces, in the case of cycloid gearing.

An advantage of the cycloidal reducer is that several teeth are always in simultaneous contact. The single conjugate pair of teeth (one pair of teeth in contact) as the most critical theoretical case was analyzed here.

Analysis was performed using a strain gauges technique [24]. Strain gauges of type 2/120 KY11 (HBM) were used. Considering the dimensions of the cycloid disc and available strain gauges, it was not possible to measure strain in the contact zone itself, but within the closest possible zone (on the tooth of the cycloid disc on which the excitation force acts and in the closest opening in the cycloid disc body where the roller of the central disc passes). Ten strain gauges in total were glued, divided into two groups with five gauges each, on a constant distance of 2 mm, which provided sufficient information about the stress distribution character.

The strain was measured for different values of static excitation force (F_N) in a range from 0 to 5200 N. Strain and stress values, which were measured and calculated for the contact force of $F_N = 5091$ N are given in Table 4. Measurements were repeated three times for each force value in order to verify the accuracy of results. Comparison between experimentally and numerically obtained stress values is shown in Table 4. The largest stress values from all ten observed zones were produced at the position of strain gauge no. 5.

4.3 Discussion. Stress distribution on elements of the newly designed two-stage cycloidal speed reducer was rather uniform and balanced. Larger stress values were obtained when machining tolerances were taken into consideration. With the increase of the number of rollers (teeth) that are simultaneously in contact and transfer load, values of maximum Von-Mises stress were decreasing (Table 2).

When the most extreme load cases were excluded, that is, when only one roller of each relevant element was in contact (one pair of teeth in contact), the eccentric was the most loaded element of the reducer. Above all, it is a consequence of its small dimensions. An additional source of stress concentration is the key seating.

It should also be emphasized that torques, as well as relevant contact forces F_{Ni} (Table 1), on cycloid discs of the first and second stage exhibited similar values. Slightly larger values of the contact forces on cycloid discs of the second stage were obtained, consequently exhibiting larger Von-Mises stress values (Fig. 8) for this disc. Good agreement of numerical and experimental

Table 4 Experimental and numerical stress values

Strain gauge	Node	ϵ , experimental value($\mu\text{m}/\text{m}$)	σ , experimental value(MPa)	σ_x (MPa)	σ_y (MPa)	σ , numerical value(MPa)	Error(%)
1	337	62	13.02	12.3	1.12	12.4	5.1
2	336	138	28.98	27.56	2.06	27.6	4.6
3	335	218	45.78	43.65	1.65	43.7	4.6
4	334	249	52.29	50.32	2.12	50.4	3.7
5	333	298	62.58	60.43	1.15	60.4	3.4
6	994	217	45.57	42.45	4.86	42.7	6.2
7	995	227	47.67	44.16	3.15	44.3	7.1
8	996	218	45.78	43.65	5.12	43.9	4.0
9	997	213	44.73	42.15	3.12	42.3	5.5
10	998	206	43.26	40.12	2.65	40.2	7.1

results of the stress state for the cycloid discs of the first stage should certainly be emphasized.

5 Conclusions

This paper presents a new concept of the two-stage cycloidal speed reducer where only one cycloid disc is used for each stage. Expressions for the torque on relevant elements of the reducer are given, as well as expressions for calculation of the contact forces on the cycloid disc teeth.

Numerical analysis of the stress state for the vital elements of the reducer (cycloid disc, central disc, stationary ring gear of the first stage, rotatable ring gear of the second stage, and eccentric) was realized. Also, experimental analysis of the stress state of the first stage cycloid disc was performed, using a strain gauges technique.

Based on the obtained results, it can be concluded that all vital elements of the reducer were uniformly loaded and the stress range provides normal work for its anticipated lifetime. It is especially important that this refers to both cycloid discs of the first and second stage, because, for this design, only one cycloid disc is used for each stage, instead of two, thus significantly decreasing reducer dimensions.

Also, the newly adopted concept has less rotating elements, so the noise is low and the effect of canceling out eccentricity vibrations is preserved.

References

- [1] Kudrijavcev, V. N., 1966, "Planetary Gear Train" (in Russian), Mech. Eng. (Leningrad).
- [2] Lehmann, M., 1976, "Calculation and Measurement of Forces Acting on Cycloid Speed Reducer (in German)," Ph.D thesis, Technical University Munich, Germany.
- [3] Malhotra, S. K., and Parameswaran, M. A., 1983, "Analysis of a Cycloid Speed Reducer," *Mech. Mach. Theory*, **18**(6), pp. 491–499.
- [4] Litvin, F., 1989, *Theory of Gearing*, NASA, Washington DC.
- [5] Blanche, J. G., and Yang, D. C. H., 1989, "Cycloid Drives with Machining Tolerances," *J. Mech. Trans. Autom. Des.*, **111**, pp. 337–344.
- [6] Yang, D. C. H., and Blanche, J. G., 1990, "Design and Application Guidelines for Cycloid Drives with Machining Tolerances," *Mech. Mach. Theory*, **25**(5), pp. 487–501.
- [7] Gu I., 1998, "Design of Antibacklash Pin-Gearing," *J. Mech. Des.*, **120**, pp. 133–138.
- [8] Demenego, A., Vecchiato, D., Litvin, F., Nervegna, N., and Manco, S., 2002, "Design and Simulation of Meshing of a Cycloidal Pump," *Mech. Mach. Theory*, **37**(8), pp. 311–332.
- [9] Litvin, F., and Feng, P., 1996, "Computerized Design and Generation of Cycloidal Gearings," *Mech. Mach. Theory*, **31**(7), pp. 891–911.
- [10] Chmurawa, M., and Lokiec, A., 2001, "Distribution of Loads in Cycloidal Planetary Gear (CYCLO) Including Modification of Equidistant," 16th European ADAMS User Conference, Berchtesgaden, Germany.
- [11] Chmurawa, M., and John, A., 2000, "Numerical Analysis of Forces, Stress and Strain in Planetary Wheel of Cycloidal Gear Using FEM," Numerical Methods in Continuum Mechanics, Liptovsky Jan, Slovak Republic.
- [12] Yan, H. S., and Lai, T. S., 2002, "Geometry Design of an Elementary Planetary Gear Train With Cylindrical Tooth Profiles," *Mech. Mach. Theory*, **37**(8), pp. 757–767.
- [13] Chen, B. K., Fang, T. T., Li, C. Y., and Wang, S. Y., 2008, "Gear Geometry of Cycloid Drives," *Sci. China E: Technol. Sci.*, **51**(5), pp. 598–610.
- [14] Hwang, Y. W., and Hsieh, C. F., 2006, "Geometry Design and Analysis for Trochoidal-Type Speed Reducers: With Conjugate Envelopes," *Trans. CSME/de la SCGM*, **30**(2), pp. 261–278.
- [15] Hwang, Y. W., and Hsieh, C. F., 2007, "Geometric Design Using Hypotrochoid and Nonundercutting Conditions for an Internal Cycloidal Gear," *J. Mech. Des.*, **129**, pp. 413–420.
- [16] Yunhong, M., Changlin, W., and Liping, L., 2007, "Mathematical Modeling of the Transmission Performance of 2K-H Pin Cycloid Planetary Mechanism," *Mech. Mach. Theory*, **42**(7), pp. 776–790.
- [17] Sensinger, J., 2010, "Unified Approach to Cycloid Drive Profile, Stress, and Efficiency Optimization," *J. Mech. Des.*, **132**, p. 024503.
- [18] Blagojević M., 2008, "Stress and Strain State of Cyclo Speed Reducer's Elements Under Dynamic Loads" (in Serbian), Ph.D thesis, Faculty of Mechanical Engineering, Kragujevac, Serbia.
- [19] Blagojević M., Nikolić, V., Marjanović, N., and Veljović, L. J., 2009, "Analysis of Cycloid Drive Dynamic Behavior," *Sci. Tech. Rev.*, **LIX** (1), pp. 52–56.
- [20] Kahraman, A., Ligata, H., and Singh, A., 2010, "Influence of Ring Gear Rim Thickness on Planetary Gear Set Behavior," *J. Mech. Des.*, **132**(2), p. 021002.
- [21] Li, X., He, W., Li, L., and Schmidt, L. C., 2004, "A New Cycloid Drive With High-Load Capacity and High Efficiency," *J. Mech. Des.*, **126**(4), pp. 683–686.
- [22] Gorla, C., Davoli, P., Rosa, F., Longoni, C., Chiozzi, F., and Samarani, A., 2008, "Theoretical and Experimental Analysis of a Cycloidal Speed Reducer," *J. Mech. Des.*, **130**(11), p. 112604.
- [23] Chen, C., Zhang, X., and Angeles, J., 2007, "Kinematic and Geometric Analysis of a Pure-Rolling Epicyclic Train," *J. Mech. Des.*, **129**(8), pp. 852–857.
- [24] Hoffmann, K., 1989, *An Introduction to Measurements Using Strain Gages* (HBM, Darmstadt, 1989).